



Supplement of

Impact of satellite viewing-swath width on global and regional aerosol optical thickness statistics and trends

P. R. Colarco et al.

Correspondence to: P. R. Colarco (peter.r.colarco@nasa.gov)

Supplementary Material

Aerosol model description and aerosol assimilation methodology

The aerosol module run inline in the Goddard Earth Observing System (GEOS-5) Earth system model (Rienecker et al., 2008) is based on the Goddard Chemistry, Aerosol, Radiation, and Transport (GOCART, Chin et al., 2002). Implementation and evaluation of GOCART in the GEOS environment is described in Colarco et al. (2010). The GOCART module treats the lifecycles—including sources, sinks, and chemistry—of tropospheric sulfate, carbonaceous, dust, and sea salt aerosols as a series of non-interacting tracers. Dust and sea salt have dynamic (wind-speed driven) emission sources. Anthropogenic aerosol and precursor sources are primarily from the AeroCom-II HCA0 emission inventory (<http://aerocom.met.no/aerocomhome.html>). Biomass burning emissions are from a MODIS fire radiative power derived emission source, and so have daily variability (Darmenov and da Silva, 2013). Utility and evaluation of this module within GEOS-5 have been reported in numerous studies (Ott et al., 2010, Nowottnick et al., 2010, 2011, Bian et al., 2012, Randles et al., 2013, Kishcha et al., 2013, Buchard-Marchant et al., 2014, Yasunari et al., 2014, Reale et al., 2014).

Based on the work of Zhang and Reid (2006) and Lary et al. (2009), a back-propagation neural network was developed to correct observational biases related to cloud contamination, surface parameterization, and aerosol microphysics in the MODIS Collection 5 AOT dataset. This empirical algorithm has been adapted to retrieve AOT directly from cloud-cleared MODIS reflectances. On-line quality control is performed with the adaptive buddy check of Dee et al. (2001), with observation and background errors estimated using the maximum likelihood approach of Dee and da Silva (1999). Following a multi-channel AOT analysis, three-

dimensional analysis increments are produced exploring the Lagrangian characteristics of the problem, generating local displacement ensembles intended to represent misplacements of the aerosol plumes.

Figure S6a shows the frequency histogram of pairwise hourly MERRAero and Level 2 (cloud-clear, quality assured) AERONET AOT comparisons for the entire analysis period (approximately 2.5 million matchups at 583 AERONET sites). Although MERRAero has a peak in the frequency histogram near the zero-bias point, it is clear that MERRAero retains a slight overall low bias relative to AERONET, particularly evident when looking at the right-hand side of the diagram, which shows the difficulty MERRAero has at representing high AOT events as observed in AERONET. MERRAero is designed to represent gridbox mean AOT, and local extrema in a gridbox are outside its “domain.” For geographic context, Figure S6b presents the same information separated by AERONET site, with the size of the symbol indicating the number of coincidences compared and the color showing the overall model bias at the site. MERRAero exhibits its strongest low-AOT biases in Brazil, the Sahel, India, and Southeast Asia, the latter two regions being places where aerosol emissions are changing rapidly (and so may not be well represented in the model yet) and aerosol retrievals from satellite have a lot of issues that would confound the benefit of the assimilation methodology. There is as well somewhat of a high bias across most of the United States and in southern South America and Australia. We do not show it here, but the skill of the MERRAero system is considerably improved with respect to AERONET versus a similar run of the GEOS-5 system that does not include the aerosol assimilation.

References

- Bian, H., P.R. Colarco, M. Chin, G. Chen, J.M. Rodriguez, Q. Liang, D. Blake, D.A. Chu, A. da Silva, A.S. Darmenov, G. Diskin, H.E. Fuelberg, G. Huey, Y. Kondo, J.E. Nielsen, X. Pan, X. and A. Wisthaler, 2013: Source attributions of pollution to the Western Arctic during the NASA ARCTAS field campaign, *Atmos. Chem. Phys.*, 13(9), 4707–4721, doi:10.5194/acp-13-4707-2013.
- Buchard, V., A.M. da Silva, P. Colarco, N. Krotkov, R.R. Dickerson, J.W. Stehr, G. Mount, E. Spinei, H.L. Arkinson, and H. He, 2014: Evaluation of GEOS-5 sulfur dioxide simulations during the Frostburg, MD 2010 field campaign, *Atmos. Chem. Phys.*, 14(4), 1929–1941, doi:10.5194/acp-14-1929-2014.
- Chin, M., P. Ginoux, S. Kinne, O. Torres, B. Holben, B. Duncan, R. Martin, J. Logan, A. Higurashi, and T. Nakajima, 2002: Tropospheric aerosol optical thickness from the GOCART model and comparisons with satellite and Sun photometer measurements, *J. Atmos. Sci.*, 59(3), 461–483.
- Colarco, P., A. da Silva, M. Chin, and T. Diehl, 2010: Online simulations of global aerosol distributions in the NASA GEOS-4 model and comparisons to satellite and ground-based aerosol optical depth, *J. Geophys. Res. Atmos.*, 115, doi:10.1029/2009JD012820.
- Darmenov, A. S., and A. da Silva, 2013: The Quick Fire Emissions Dataset (QFED) - Documentation of versions 2.1, 2.2 and 2.4, *NASA Technical Report Series on Global Modeling and Data Assimilation*, ed. M.J. Suarez, 32, 1–183.
- Dee, D., and A. da Silva, 1999: Maximum-likelihood estimation of forecast and observation error covariance parameters. Part I: Methodology, *Mon. Weather. Rev.*, 127(8), 1822–1834.

Dee, D., L. Rukhovets, R. Todling, A. da Silva, and J. Larson, 2001: An adaptive buddy check for observational quality control, *Q. J. Roy. Meteor. Soc.*, 127(577), 2451–2471.

Kishcha, P., A.M. da Silva, B. Starobinets, and P. Alpert, 2013: Air pollution over Northwest Bay of Bengal in the early post-monsoon season: Evaluating the NASA MERRAero assimilated datasets. *J. Geophys. Res.* **119**, doi:10.1002/ 2013JD020328.

Lary, D. J., L.A. Remer, D. MacNeill, B. Roscoe, and S. Paradise, 2009: Machine learning and bias correction of MODIS aerosol optical depth, *Geosci. Rem. Sens. Lett.*, IEEE, 6(4), 694–698.

Nowottnick, E., P. Colarco, R. Ferrare, G. Chen, S. Ismail, B. Anderson, and E. Browell, 2010: Online simulations of mineral dust aerosol distributions: Comparisons to NAMMA observations and sensitivity to dust emission parameterization, *J. Geophys. Res. Atmos.*, 115, doi:10.1029/2009JD012692.

Nowottnick, E., P. Colarco, A. da Silva, D. Hlavka, and M. McGill, 2011: The fate of Saharan dust across the Atlantic and implications for a Central American dust barrier, *Atmos. Chem. Phys.*, 11(16), 8415–8431, doi:10.5194/acp-11-8415-2011.

Ott, L., B. Duncan, S. Pawson, P. Colarco, M. Chin, C. Randles, T. Diehl, and E. Nielsen, 2010: Influence of the 2006 Indonesian biomass burning aerosols on tropical dynamics studied with the GEOS-5 AGCM, *J. Geophys. Res. Atmos.*, 115, doi:10.1029/2009JD013181.

Randles, C. A., P.R. Colarco, and A. da Silva, 2013: Direct and semi-direct aerosol effects in the NASA GEOS-5 AGCM: Aerosol-climate interactions due to prognostic versus prescribed aerosols, *J. Geophys. Res. Atmos.*, 118, doi:10.1029/2012JD018388.

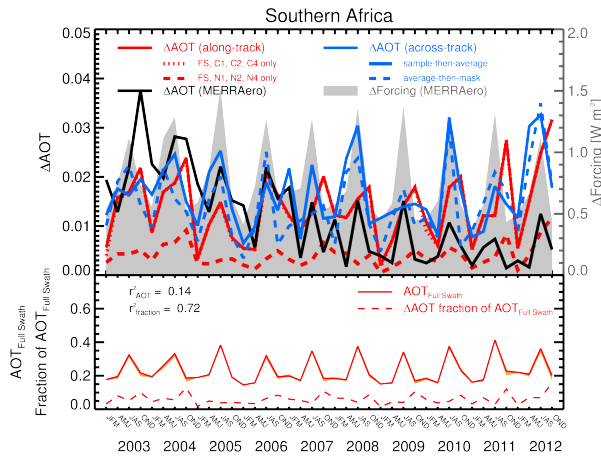
Reale, O., K.-M. Lau, A. da Silva, and T. Masui, 2014: Impact of assimilated and interactive aerosol on Tropical Cyclogenesis. *Geophys. Res. Lett.* In press.

Rienecker, M., M. Suarez, R. Todling, J. Bacmeister, L. Takacs, H.C. Liu, W. Gu, M. Sienkiewicz, R. Koster, R. Gelaro, I. Stajner, and J. Nielsen, 2008: The GEOS-5 Data Assimilation System--Documentation of Version 5.0.1, 5.1.0, and 5.2.0, *NASA Technical Report Series on Global Modeling and Data Assimilation*, ed. M.J. Suarez, 27, 1–118.

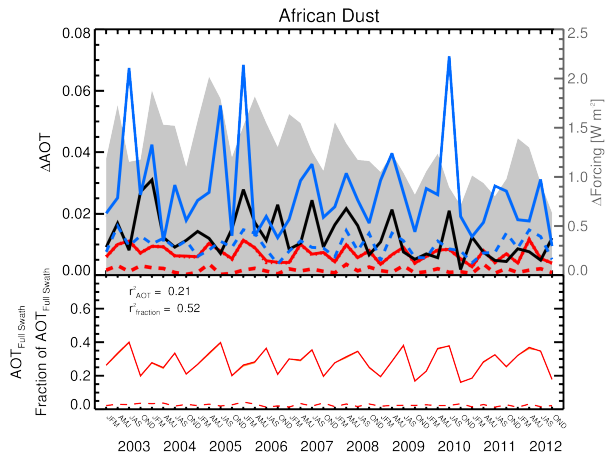
T. J. Yasunari, K.-M. Lau, S. P. P. Mahanama, P. R. Colarco, A. M. da Silva, T. Aoki, K. Aoki, N. Murao, S. Yamagata, and Y. Kodama, 2014: The GOddard SnoW Impurity Module (GOSWIM) for the NASA GEOS-5 Earth System Model: Preliminary comparisons with observations in Sapporo, Japan. *Sci. On-line Lett. Atmos.* **10**, 50–56, doi:10.2151/sola.2014-011

Zhang, J., and J.S. Reid, 2006: MODIS aerosol product analysis for data assimilation: Assessment of over-ocean level 2 aerosol optical thickness retrievals, *J. Geophys. Res. Atmos.*, **111**(D22), D22207, doi:10.1029/2005JD006898.

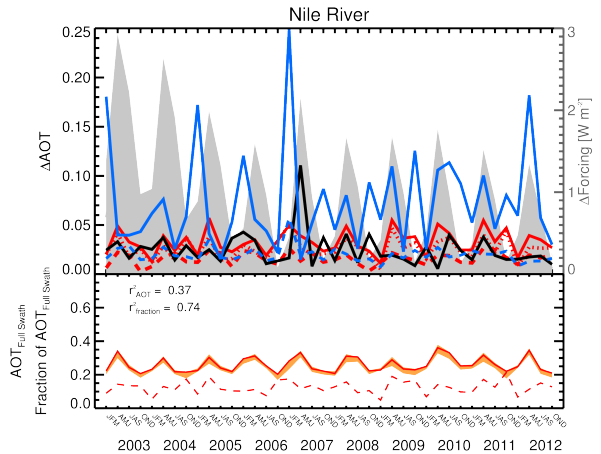
(a)



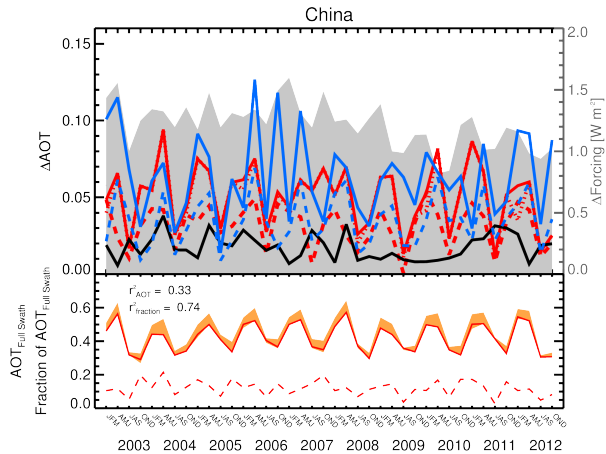
(b)



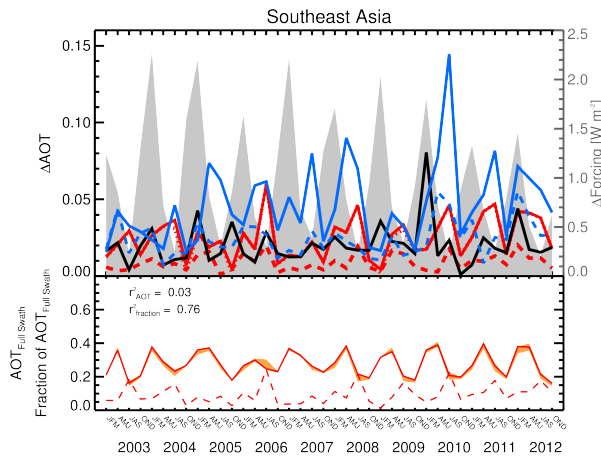
(c)



(d)



(e)



(f)

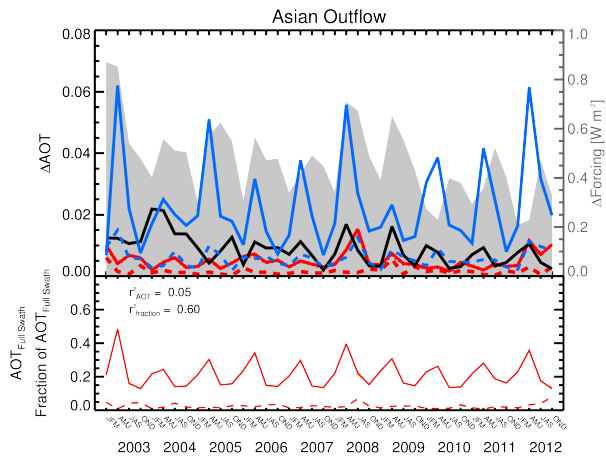


Figure S1. As in Figures 9 and 10, but for (a) Southern Africa, (b) African Dust, (c) Nile River, (d) China, (e) Southeast Asian, and (f) Asian Outflow regions.

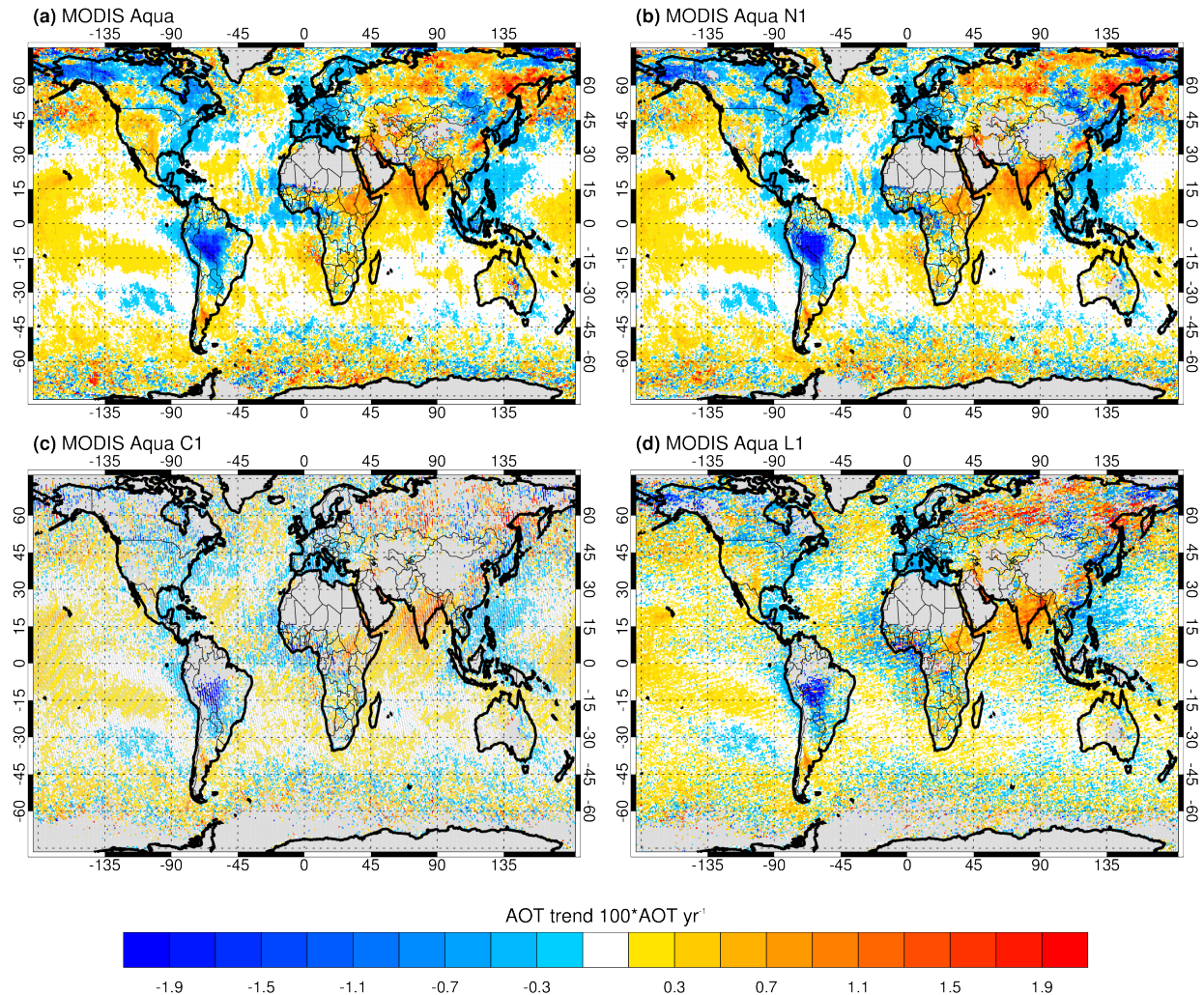


Figure S2. As in Figure 11, trend for the ten-year (2003 – 2012) time series of MODIS Aqua AOT for the (a) full swath, (b) N1, (c) C1, and (d) L1 samplings. Trends are computed following the “average-then-mask” method. Grey areas are locations with either no valid retrievals or where the time series has fewer than 12 month_n and month_{n-1} pairs.

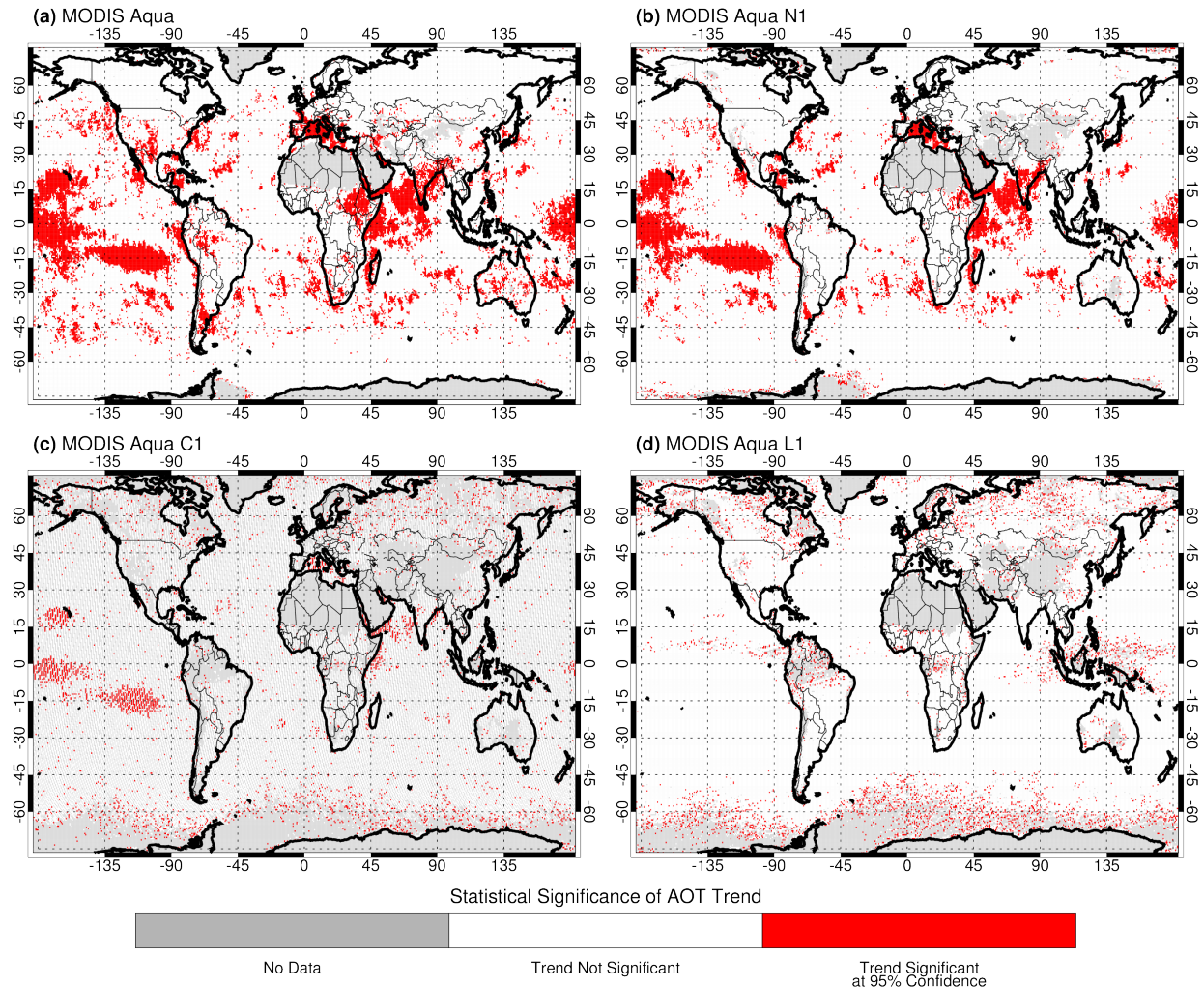


Figure S3. Statistical significance of the trends shown in Figure S2, computed from the “average-then-mask” method.

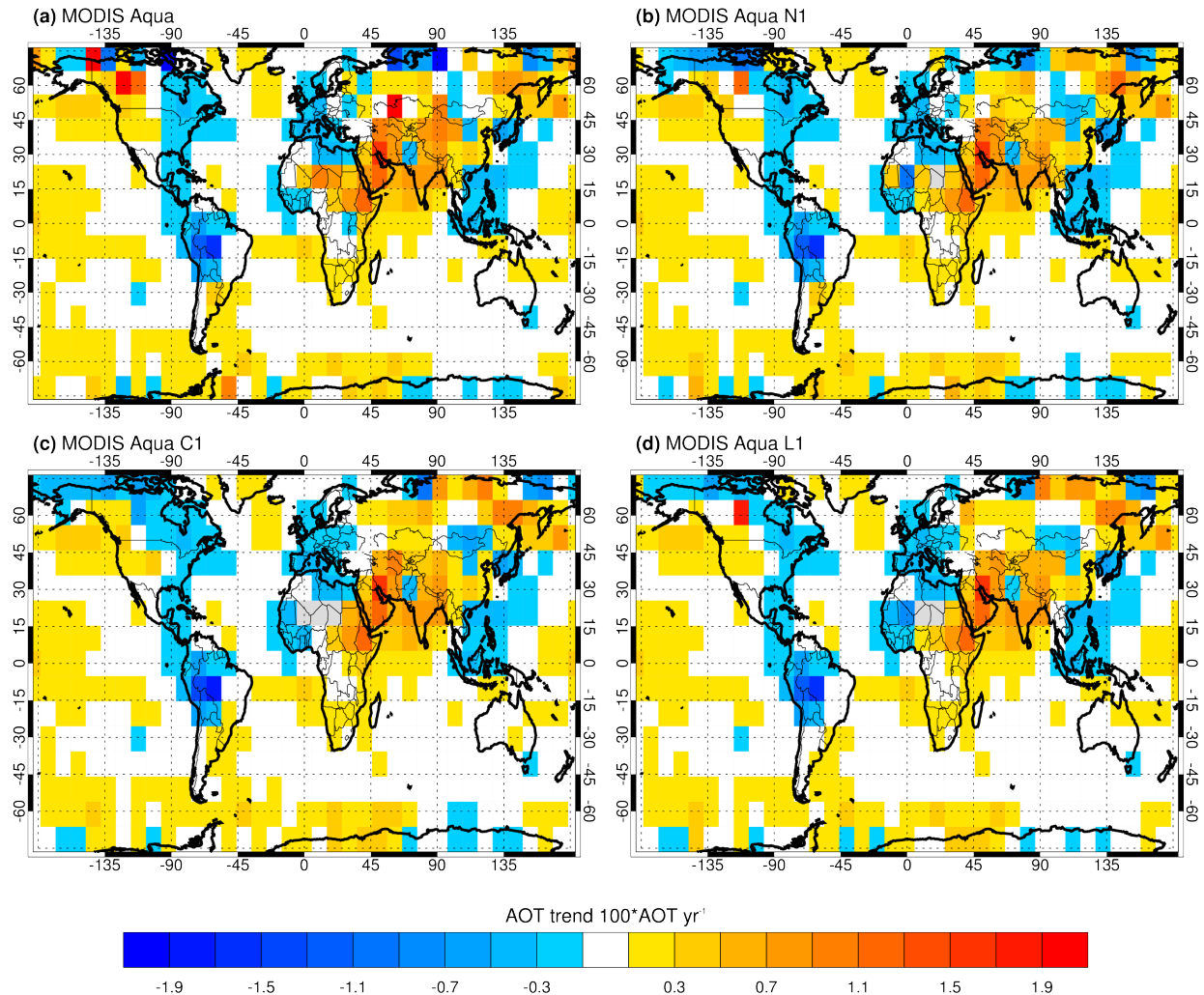


Figure S4. As in Figure 14, but showing the coarse resolution trends calculated using the “average-then-mask” approach.

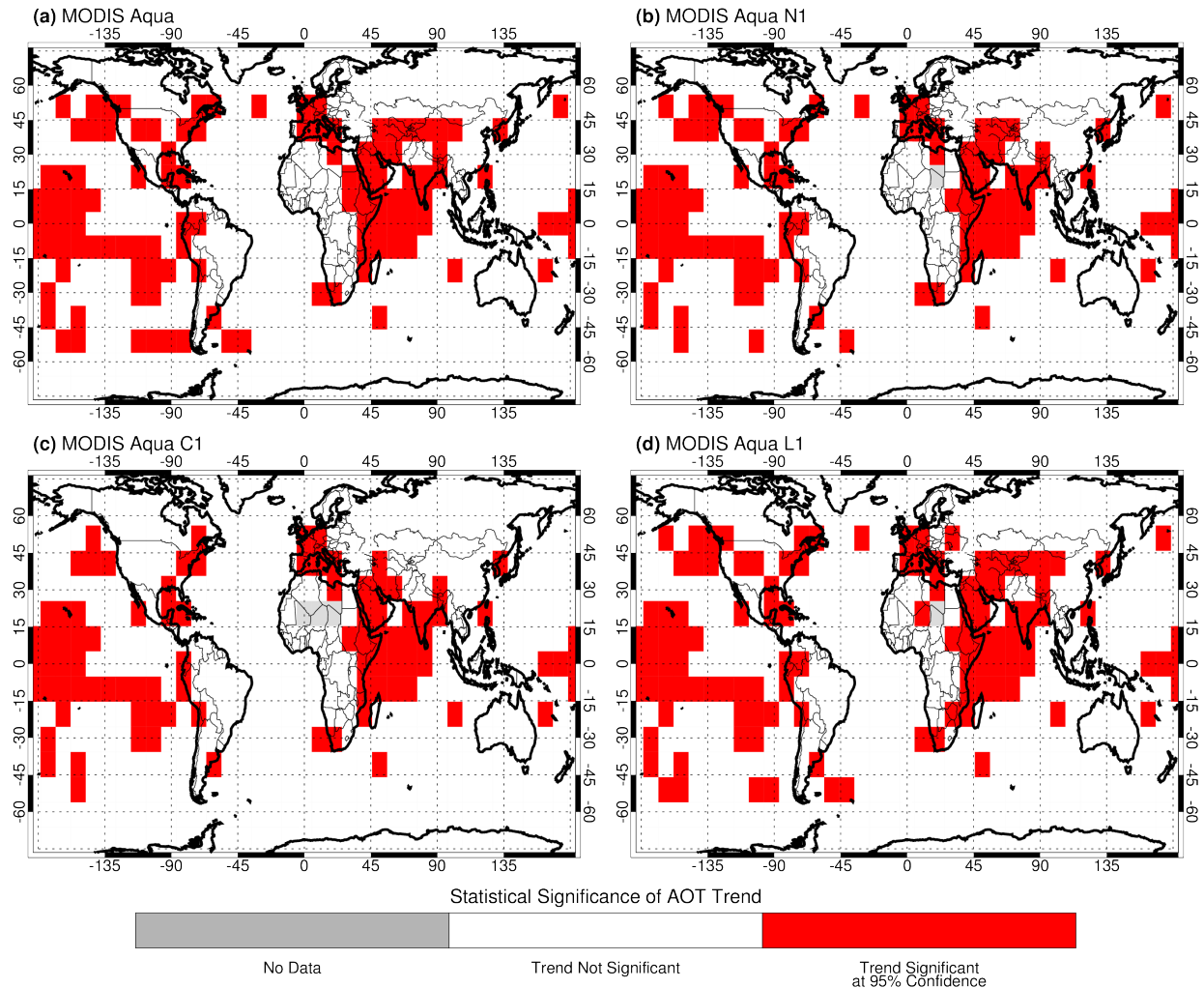


Figure S5. As in Figure 15, but showing statistical significance of coarse resolution trends computed using the “average-then-mask” approach.

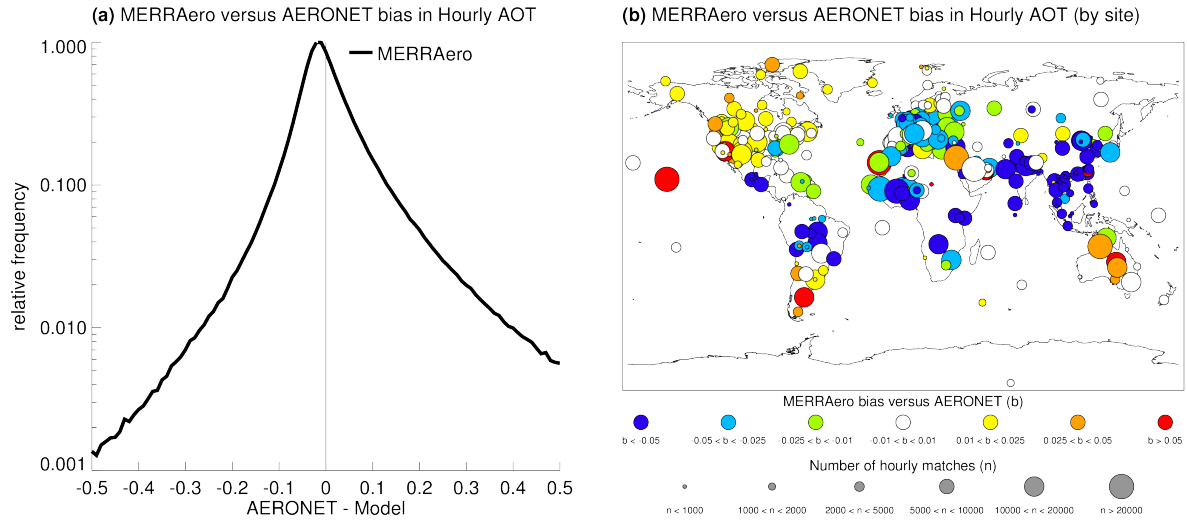


Figure S6. Comparison of MERRAero hourly AOT [550 nm] to coincident AERONET observations over the period 2003 – 2012. (a) Frequency histogram of (AERONET – Model) AOT differences. (b) Map showing locations of AERONET sites used, shading and diameter of symbols indicating, respectively, MERRAero bias and number of hourly match-ups over the ten-year comparison period.